UCRL-17509

eg. 2

University of California

Ernest O. Lawrence Radiation Laboratory

RESONANCE DESTRUCTION OF ANGULAR CORRELATIONS: ^{100}Rh IN Fe AND Ni

E. Matthias, D. A. Shirley, N. Edelstein,
H. J. Körner, and B. A. Olsen

July 1967

DISCLAIMER

Paper for the International Conference on Hyperfine Interactions Detected by Nuclear Radiation
August 25-30, 1967, Asilomar, California

UCRL-17509
Preprint

UNIVERSITY OF CALIFORNIA

Lawrence Radiation Laboratory
Berkeley, California

AEC Contract No. W-7405-eng-48

RESONANCE DESTRUCTION OF ANGULAR CORRELATIONS: ^{100}Rh IN Fe AND Ni

E. Matthias, D. A. Shirley, N. Edelstein, H. J. Körner, and B. A. Olsen

July 1967

UCRL-17509

RESONANCE DESTRUCTION OF ANGULAR CORRELATIONS: ^{100}Rh IN Fe AND Ni*

E. Matthias, D. A. Shirley, N. Edelstein, H. J. Körner,† and B. A. Olsen‡

Department of Chemistry and
Lawrence Radiation Laboratory
University of California
Berkeley, California

July 1967

ABSTRACT

NMR absorption in the 235 nsec state of ^{100}Rh has been detected by angular correlations, employing the hyperfine fields of Rh in Fe and Ni. Dependence of the resonance effect on rf power and polarization of the host foil has been studied. The observed line width as well as the power dependence can be qualitatively understood by comparison with theoretical expectations. Evidence for localized moments is found from the temperature variation of the resonance frequency. A possible ^{100m}Rh - ^{103}Rh hyperfine anomaly is discussed.

*This work supported by the U. S. Atomic Energy Commission.

†Summer visitor 1966, permanent address: Physik-Department der Technischen Hochschule, Munich, Germany.

‡Visitor, permanent address: Institute of Physics, Uppsala, Sweden.

I. INTRODUCTION

Perturbed angular correlations have been increasingly used for the determination of magnetic hyperfine fields of impurity atoms in ferromagnetic lattices.[1] Most of the measurements have been carried out in a time-integral manner using nuclear states with lifetimes shorter than a few nanoseconds. The accuracy of such integral measurements is limited by the fact that only the product $g \cdot H_{eff} \cdot \tau$ can be obtained. Both the nuclear g-factor, g, and the lifetime, τ, must be known with good accuracy in order to deduce the effective field, $\vec{H}_{eff}=\vec{H}_0'+\vec{H}_{int}$, with reasonable precision. Here $\vec{H}_0'$ is the external polarizing field and $\vec{H}_{int}$ is defined as the sum of the hyperfine field, the demagnetization field, and the Lorentz field, $\vec{H}_{int}=\vec{H}_{hf}-D\vec{M}+4\pi/3\ \vec{M}$. The accurate knowledge of τ is no longer required if it is sufficiently long to permit time-differential investigations, which measure the quantity $g \cdot H_{eff}$. Time-differential determinations of hyperfine fields have been carried out only with the cases of ^{19}F[2], ^{99}Ru, and ^{111}Cd [3]. The applicability of this type of measurement is limited by the electronic time resolution and by the nuclear lifetime, which provides a natural time window. Thus, very small or very large interaction frequencies cannot be observed time-differentially. Since hyperfine fields are usually fairly large, this constitutes a severe practical limitation for this technique. At first glance, the 74.8-keV state in ^{100}Rh $(T_{1/2}=235\ ns)$[4] appears to be a favorable candidate for time-differential measurements. The large g-factor of this state $(g=2.15)$[4], however, gives even for Rh in Ni a precession time of 1.5 nsec for one wavelength ($\frac{1}{2} T_L=2\pi(g \cdot H_{eff} \cdot \mu_N/\hbar)^{-1}$), which cannot be resolved with standard timing techniques. The spin rotation for Rh in Co or Fe would be still faster,

and the question arises whether it is at all possible to measure large hyperfine interactions accurately with angular correlations.

The realization that NMR-spectra and time-spectra of spin rotations are Fourier transforms of each other points toward a solution: a sufficient number of spin rotations has a well-defined frequency transform. This means, if the spin rotations can no longer be resolved in the time spectrum it should be possible to perform a resonance experiment, in which the large hyperfine field can be used to drive the resonance[5].

The possibility of an angular correlation-NMR experiment was suggested by Abragram and Pound[6] and the first successful measurement of this type was carried out with the 74.8-keV state of ^{100}Rh in a nickel lattice[7]. In this paper we give a more detailed report on further experiments and calculations involving angular correlation-NMR. The resonance effect for ^{100}Rh in Fe is discussed in Sec. II together with the power dependence and the magnetic saturation behavior of the sample. In Sec. III a redetermination of the resonance for ^{100}Rh in Ni is described. Section IV gives a brief theoretical outline of the resonance effect in angular correlations. A summary and future prospects of this method are discussed in Sec. V.

II. RHODIUM-100 IN Fe

The first experiment in which the large hyperfine field in a ferromagnetic lattice was used to achieve a resonance destruction of an angular correlation raised many questions which demanded further investigation of this effect. The following points are of interest:

1. Expected magnitude of the resonance effect;
2. Interpretation of the observed line width;
3. Power dependence of the resonance effect;
4. Favorable geometries.

To solve these problems experiments were carried out with the 84-74.8 keV cascade in ^{100}Rh, which has a large positive anisotropy and whose intermediate state has a half-life of 235 nsec and a g-factor of 2.15 [4]. The geometry for such a resonance experiment is shown in Fig. 1. The detectors were placed at $\theta=180°$. A thin foil of the ferromagnetic material into which the activity had been diffused was mounted with its plane parallel to the dc field and to the (common) axis of both detectors. The polarizing field, H_0', applied parallel to this axis insures, in saturation, a completely decoupled, unperturbed angular correlation. The rf-field, H_1', has to be applied perpendicular both to the detector plane and consequently, to H_0'. In all measurements described below 3"×3" NaI(Tl) detectors were used at a distance of 10 cm. Since the detectors do not resolve γ_1 and γ_2, both were taken together in the window of each single channel.

A ferromagnetic host had been chosen to take advantage of the enhancement factor that it provides for NMR absorption. For half-lives below 1 msec

this is necessary to meet the power requirement for this type of experiment unless one employs a more elaborate pulsed-rf technique. The amplitude enhancement of the externally applied rf field[5] (valid for domains only),

$$2H_1 = (1+\frac{H_{hf}}{H_0'})H_1' \qquad (1)$$

indicates the advantage of large internal fields for NMR experiments. For the study of the resonance mechanism we therefore concentrated on ^{100}Rh in Fe. Figure 2 shows the result of a 5-hr frequency scan at room temperature, yielding an interaction frequency of 882.7±2.0 MHz.

Since all sources were prepared by electroplating ^{100}Pd carrier-free onto foils of about 10^{-4} cm thickness[8] and subsequently diffusing the activity for at least 12 hrs at 950°C, we found it desirable to check the reproducibility of this procedure. The results obtained with three different sources, rf-coils, and power levels are listed in Table I. The agreement among the three measurements is satisfactory and provides trust in the method used for source preparation.

The question of whether the resonance is observed in walls or domains can be answered by measuring the magnetic saturation behavior of the foil. In Fig. 3 the coincidence counting rate at 180° is shown as a function of the polarizing field, both without and with rf-field (at resonance). The foil appears to be saturated at about 400 gauss in both cases. The resonance effect, i.e., the difference between the two curves, is largest in the range near 200 gauss. We attribute the decrease of the resonant effect with field to the decreasing

enhancement factor (Eq. (1)). In contrast to conventional NMR a clear differentiation between wall and domain resonances is impossible with the present technique. Diffusion, solution, or implantation processes do not discriminate against either walls or domains and the radioactive atoms are in all likelihood homogeneously distributed throughout the sample. Therefore, even at very small fields, one expects to see a net effect which originates from nuclei both in walls and domains. However, we can establish in two independent ways that the observed resonance takes place in domains: (1) The magnitude of the resonant effect is much too large to arise in walls. First, the nuclei in walls are randomly polarized and contribute to the angular correlation only the "hard core" value, $A_2/5$ [9]. At resonance this hard core is reduced by merely a small fraction, due to the fact that only few nuclei happen to be oriented parallel or antiparallel to the observation direction of the γ rays. Second, only a small fraction ($\lesssim 5\%$) of the ^{100}Rh nuclei are expected to be in walls if the ^{100}Pd parent is randomly distributed in the sample. However large the amplitude of H_1' may be, if the criterion $H_1' \ll H_0'$ is maintained, and if H_0' is insufficient to sweep out the walls completely, then the amplitude of wall motion can be only of the order of the wall thickness, δ, and only a fraction δ/ℓ, where ℓ is the domain width, of ^{100}Rh nuclei can be affected. The rest will add to the nonresonant background, and a wall resonance has thus an upper amplitude limit of $\sim 1/5\ A_2(\delta/\ell) \ll 1\%$.

(2) The survival of an effect after the foil is saturated is possible only for domain resonance, as the walls are gone.

The only well defined resonance is obtained with a magnetically saturated foil, free of walls. From the nuclear point of view it is this domain resonance which is of interest since it allows us to measure the g-factor directly by observing the linear relationship between resonance frequency and external field.

At first sight the effects shown in Fig. 3 seem unduly small for a case with A_2=0.175, but they are actually about as expected, in light of several geometrical factors. It is important to understand these factors because then by comparing theory with experiment we can decide unambiguously what fraction of the radioactive nuclei in a specimen are actually contributing to a given resonance. A rigorous theory is developed in Sec. IV. We can, however, get a general impression of the expected magnitudes of the effects shown in Figs. 3 and 4 (where the power dependence is shown) from simple considerations. With H_0'=0 and H_1'=0 we have the random fields case[9], and

$$\overline{W(\pi)} = 1+\sum_k \frac{1}{(2k+1)} Q_k A_k$$

For this case Q_2 (the solid angle correction) is 0.81, A_2=0.175, $A_{k>2}$=0, and $\overline{W(\pi)}$ = 1.028. As H_0' (directed along the γ-ray direction) is raised, $\overline{W(\pi)}$ rises to

$$\overline{W(\pi)} = 1+\sum_k Q_k A_k$$

or 1.142, an increase of 11.1%. The experimental increase of 8% (Fig. 3) is consistent with this if we remember that considerable scattering and absorption

takes place at the rf coil surrounding the source and at the associated magnetic field coil (see Fig. 1).

On application of the rf field at resonance, $\overline{W(\pi)}$ should drop from $1+Q_2A_2$ to the "hard-core" value $1+1/4\ Q_2A_2$ (Sec.IV), in this case by 9.3%. Although the hard-core was not completely reached, the observed decrease of 6.9% (Fig. 4) is consistent with this figure, considering that the decoupling effect, also was attenuated by about 3.4%. The maximum power point (at 2.15 volts) in Fig. 4 corresponds to 100 watts. This seems to saturate the resonance. The fact that this saturation value is still well above $\overline{W(\pi)}=1$ confirms the theoretical prediction of a hard-core value for this geometry (Sec. IV).

The run with source no. 2 (displayed in Fig. 5) was judged to give the most reliable value of the frequency: it was used to evaluate the hyperfine field for ^{100}Rh in Fe at room temperature. With a g-factor of g=2.15 the field is

$$H_{hf}(T=300^\circ K) = 538.0\pm0.6 \text{ kG} \quad .$$

From Fig. 5 it appears that the shape of the resonance is symmetric and there is no evidence for more than one magnetic site for the ^{100}Rh. The line-width is in all three cases large compared to the natural width $\Delta\nu=1/2\pi\tau_N=0.47$ MHz. This point will be discussed in Sec. IV.

The shift of the resonance due to the temperature dependence of the hyperfine field is also demonstrated in Fig. 5. The resonance at 77°K is shown in the lower part, and is compared to the data of the upper part, which

were observed at room temperature. The resonance frequency for 77°K is listed under run 4 in Table I. It leads to a hyperfine field of

$$H_{hf}(T=77°K) = 556.8 \pm 0.6 \text{ kG}$$

For Rh in iron the large frequency shift between 300°K and 77°K indicates that the magnetization of the Rh atom drops off about 1.7 times as rapidly with increasing temperature as does the lattice magnetization. Such weak coupling to the lattice is often interpreted as indicating a localized moment[10] on the solute atom. The more complete data for ^{99}Ru in nickel[3] suggest a localized moment for that case, therefore a similar behavior was expected for the neighboring Rh in Fe.

Our extrapolated value H_{hf}(Rh in Fe, 0°K) = 559.6±0.6 kOe appears to disagree with the value 543 kOe reported by Kontani and Itoh.[11] However, we believe that this discrepancy is not real, but that it arises from a hyperfine anomaly. In future accurate comparisons of hyperfine fields obtained from different isotopes and excited states this factor will have to be considered (it can also be used to ascertain what fraction of H_{hf} arises from contact interaction). We therefore correct for the anomaly by a method that has proved successful before.[12,13] The apparent hyperfine fields obtained from ^{100}Rh and ^{103}Rh are related by[12]

$$H_{hf}^{(103)} = H_{hf}^{(100)} \frac{1+\epsilon_{103}}{1+\epsilon_{100}} \qquad (2)$$

where ϵ - the fractional hyperfine-interaction reduction - may be calculated from published tables[14] if assignments are available for the nuclear states. The hyperfine anomaly is defined as

$$^{103}\Delta^{100} = \frac{1+\epsilon_{103}}{1+\epsilon_{100}} - 1 \qquad (3)$$

For this case the magnetic moments of the 74.8-keV state of ^{100}Rh and the ground state of ^{103}Rh are believed to arise mostly from proton $g_{9/2}$ and $p_{1/2}$ orbitals, respectively. This is also the case for the ^{110m}Ag - ^{109}Ag pair, for which an anomaly of -3.7±1.0% was estimated[12], and an anomaly of $^{110m}\Delta^{109}$ = -2.5% observed[13]. There are several possible semi-empirical procedures for estimating the anomaly for the ^{100}Rh - ^{103}Rh pair, all of which yield values of $^{103}\Delta^{100} \simeq$ -3% which leads to

$$H_{hf}(103) = 0.97 H_{hf}(100m) = 542 \text{ kOe},$$

in very good agreement with experiment.

III. RHODIUM-100 IN Ni

The experiment with the ^{100}Rh in Ni source was performed to study further the resonance observed earlier in this alloy.[7] The source was prepared in the same way as for the ^{100}Rh in Fe measurements, by plating the carrier-free ^{100}Pd activity on a Ni foil, approximately 10^{-4} cm thick. The diffusion was carried out at 915°C for 20 hrs and thereafter at 975°C for 15 hrs. In the mounting of the source, provision was made for much better temperature control than in the earlier experiment.[7]

As shown in Fig. 6, it was possible to resolve the earlier-observed asymmetry of the resonance into two lines of unequal intensity. The two resonances are centered around 315.5 MHz and 334.2 MHz, corresponding to fields of 197.0 kG and 209.5 kG. The frequency shift between the main peak in Fig. 5 and the one obtained earlier[7] (322.5 MHz) is caused partly by the fact that the original value represents an average over the asymmetric resonance shape and partly by a temperature shift. In the first measurement the sample was probably at slightly higher than room temperature. The amplitude of the observed effect (1.8%) is identical with the earlier measured one in Fig. 2 of ref. 7.

Since the lines for ^{100}Rh in Ni are very broad and shallow this makes their study difficult. Two conclusions, however, seem to be justified. First, the Rh-atoms are located at two different magnetic sites with corresponding hyperfine fields of 197.0 kG and 209.5 kG. Second, a relaxation process is strongly indicated since the line width is about three times larger than for the ^{100}Rh in Fe (compare with Fig. 5) which, as we show in Sec. IV, has about

the theoretically-expected line width. This relaxation process is probably associated with a localized moment on the rhodium atom in nickel, which would make spin-lattice relaxation anomalously fast.[15]

However, a reliable interpretation can hardly be based on this one observation at room temperature only and the necessity of studying the behavior of the resonance as a function of both temperature and external field is obvious. It also would be interesting to see whether the results obtained with ^{100}Rh in Ni can be reproduced by conventional NMR using ^{103}Rh. This has to be done with an isotopically enriched even-$^{\text{mass}}$/Ni-sample, however, since the resonance of naturally abundant nickel coincides with the lower one of the two expected frequencies for ^{103}Rh in Ni[16].

IV. FORMALISM TO DESCRIBE ANGULAR CORRELATION-NMR

The experimental results obtained for ^{100}Rh in Fe raise the necessity to discuss briefly the theoretical expectations for line width, line shape and size of resonance effect. In the following the formalism leading to these predictions is derived only for a time-integral correlation function and the special geometry sketched in Fig. 1:

$$\vec{H}_0 \| \vec{\gamma}_1 (180°) \vec{\gamma}_2 \perp \vec{H}_1 \quad . \tag{4}$$

In the following we use the notation $\vec{H}_1$ and $\vec{H}_0$ for the <u>effective</u> ac- and dc-fields acting on the nuclear moment.

It is obvious that the detection of the resonance by an angular correlation introduces an additional direction not encountered in conventional NMR experiments. As a consequence, the form of the resonance depends not only upon the angle between γ_1 and γ_2 but also upon the relative orientations of H_0 and H_1 with respect to the detector plane.

The formalism to describe the resonance destruction has to be developed from the general expression for a perturbed angular correlation. A γ-ray cascade influenced by extranuclear fields and studied with detectors at angles (θ_1, ϕ_1) and (θ_2, ϕ_2) with respect to the quantization axis can be described by the correlation function[9]

$$\hat{W}(\vec{k}_1,\vec{k}_2) = \sum_{\substack{k_1 k_2 \\ N_1 N_2}} A_{k_1}(1) A_{k_2}(2) \hat{G}^{N_1 N_2}_{k_1 k_2} [(2k_1+1)(2k_2+1)]^{-1/2} Y^{N_1 *}_{k_1}(\theta_1,\phi_1) Y^{N_2}_{k_2}(\theta_2,\phi_2) \qquad (5)$$

with the usual definition of $A_{k_1}(1)$ and $A_{k_2}(2)$. The time-integral perturbation factor is defined as

$$\hat{G}^{N_1 N_2}_{k_1 k_2} = [(2k_1+1)(2k_2+1)]^{1/2} \sum_{\substack{m_a m_b \\ m_a' m_b'}} (-1)^{2I+m_a+m_b} \begin{pmatrix} I & I & k_1 \\ m_a' & -m_a & N_1 \end{pmatrix} \begin{pmatrix} I & I & k_2 \\ m_b' & -m_b & N_2 \end{pmatrix}$$

$$\times \frac{1}{\tau} \int_0^\infty e^{-t/\tau} \langle m_b | e^{-(i/\hbar)\int \mathcal{H}(t)dt} | m_a \rangle \langle m_b' | e^{-(i/\hbar)\int \mathcal{H}(t)dt} | m_a' \rangle^* dt \,. \qquad (6)$$

The interaction Hamiltonian is time-dependent and, if we chose the quantization axis (z-axis) to be parallel to $\vec{H}_0$, has the form well-known from NMR-theory[17]

$$\mathcal{H}(t) = -\gamma\hbar[H_0 I_Z + H_1(I_x \cos\omega t \pm I_y \sin\omega t)] \quad [18] \,, \qquad (7)$$

where $\gamma = g \cdot \mu_N/\hbar$, and g is the nuclear g-factor. Instead of solving the integral, the time dependence of $\mathcal{H}(t)$ can be eliminated by transforming to a coordinate system which rotates about H_0(z-axis) with frequency ω. With $\vec{H}_1$ along the x-axis we get a transformed (effective) Hamiltonian[17]

$$\mathcal{H}' = -\gamma\hbar[(\omega/\gamma \pm H_0)I_Z + H_1 I_x] \quad . \tag{8}$$

This transformation is described by the factor $\exp(\mp iN_2\,\omega t)$ which has to be multiplied into the perturbation factor.

The special choice of a geometry in which the z-axis ($\vec{H}_0$) coincides with the emission direction of γ_1 ($\Theta_1=0°$ and $\Theta_2=180°$) leads to $N_1=N_2=0$ and, consequently, $m_a=m_a'$ and $m_b=m_b'$. Thus, in this case the transformation into a rotating coordinate system affects only the interaction Hamiltonian, as the angular correlation function is invariant against rotations about the emission directions of either γ_1 or γ_2. It follows that the time-integrated angular correlation influenced by a destructive rf-field according to Fig. 1 is described by

$$\hat{W}(180°) = \sum_{k_1 k_2} A_{k_1}(1)\, A_{k_2}(2) \cdot \hat{G}^{00}_{k_1 k_2} \quad , \tag{9}$$

with

$$\hat{G}^{00}_{k_1 k_2} = [(2k_1+1)(2k_2+1)]^{1/2} \sum_{m_a m_b} (-1)^{2I+m_a+m_b} \begin{pmatrix} I & I & k_1 \\ m_a & -m_a & 0 \end{pmatrix} \begin{pmatrix} I & I & k_2 \\ m_b & -m_b & 0 \end{pmatrix}$$
$$\times \frac{1}{\tau} \int_0^\infty e^{-t/\tau} |\langle m_b | e^{-(i/\hbar)\mathcal{H}'t} | m_a \rangle|^2 \, dt \quad . \tag{10}$$

The "effective" Hamiltonian in the rotating frame (Eq.(8)) is not diagonal in the m-representation and has to be diagonalized by a unitary transformation[9]

$$U\, e^{-(i/\hbar)\,\mathcal{H}'t}\, U^{-1} = e^{-(i/\hbar)Et} \tag{11}$$

If E_n are the eigenvalues and $\langle n|m\rangle$ the corresponding eigenvectors of the interaction Hamiltonian, $\mathcal{H}'$, the time-integral perturbation factor in Eq. (10) can be expressed in the form

$$\hat{G}^{00}_{k_1 k_2} = [(2k_1+1)(2k_2+1)]^{1/2} \sum_{\substack{m_a m_b \\ n\ n'}} (-1)^{2I+m_a+m_b} \begin{pmatrix} I & I & k_1 \\ m_a & -m_a & 0 \end{pmatrix} \begin{pmatrix} I & I & k_2 \\ m_m & -m_b & 0 \end{pmatrix} \tag{12}$$

$$\times \langle n|m_b\rangle^{*}\langle n|m_a\rangle\langle n'|m_b\rangle\langle n'|m_a\rangle^{*}\{1+[(E_n-E_{n'})\tau/\hbar]^2\}^{-1} \quad .$$

This equation is best solved by numerical methods for a certain set of parameters characteristic of the experimental conditions.

The behavior of the resonance is illustrated in Figs. 7, 8, and 9 for a nuclear spin I=2 which corresponds to the ^{100}Rh case. Figure 7 shows the resonance effect for some realistic values of the parameters $\omega_0\tau$ and $H_1/H_0=10^{-3}$. The negative sign of $\omega_0\tau$ originates from the fact that the calculations were performed for one circular polarization direction only (plus sign in Eq. (8)). It is apparent that the perturbing effect of the rf-field vanishes for $\omega \ll -\omega_0$ and H_1/H_0 constant. Further, the effect is measurable only for $|\omega_0\tau| \gg 1$. For ^{100}Rh in Fe at room temperature we have $|\omega_0\tau| \simeq 1.9 \times 10^3$ which corresponds to $\hat{G}^{00}_{22} \simeq 0.25$ for a power level of $H_1/H_0=10^{-3}$.

A notable feature of the resonance behavior for k=2 is that the line is split in two minima, symmetric about the resonance frequency. In general, the resonance of G_{kk}^{00} shows a fine structure consisting of k minima. This is a remarkable feature which is encountered always when the resonance is detected by means of an anisotropic radiation field. In conventional NMR where the macroscopic susceptibility is measured this effect does not occur. Another consequence of the complex structure of the resonance is that the width increases with increasing k for a fixed power level.

It is now of interest to see how the resonance effect varies with rf-amplitude. Figure 8 shows the power dependence at resonance ($\omega=-\omega_0$). The most remarkable result of this figure is the occurrence of a "hard-core" value. Even for very large power levels the anisotropy cannot be wiped out completely but remains at a value of

$$G_{22}^{0}(\infty) = 1/4 \quad .$$

Analytically, the hard core value is given by the relation

$$G_{kk}^{00}(\infty) = (k!)^2/(k!!)^4 \quad , \qquad (13)$$

and is independent of the nuclear spin, as expected for a purely magnetic interaction.[19] It should be noticed, however, that the "hard-core" value is a geometry effect and exists only for $N_2=0$ terms. If $N_2\neq 0$, which happens for any angle $\Theta\neq 0°, 180°$, the factor $\exp(\mp iN_2\omega t)$ describing the rotating coordinate

system enters. This leads to a perturbation factor of the form

$$G_{k_1 k_2}^{N_1 N_2} \propto \frac{1}{1+\left(\frac{\tau}{\hbar}(E_n - E_{n'}) \pm N_2 \omega\tau\right)^2} \qquad (14)$$

which clearly does not exhibit a hard-core behavior for large amplitudes $H_1(\omega_1\tau \gg 1)$. The geometrical nature of the hard core effect has the consequence that it occurs only at the exact resonance frequency ω_0. Slightly to the left and right of ω_0 G_{kk}^{00} does become zero for a sufficiently large power level, as shown in Figs. 7 and 9.

For maximum power in Fig. 4 and a polarizing field of 400 G, an experimental ratio of $H_1/H_0 \simeq 2 \times 10^{-3}$ was achieved. From Fig. 8 it can be seen that this was close to saturation for $|\omega_\tau{}_0| \simeq 1.9 \times 10^3$ in agreement with the experimental behavior in Fig. 4.

After the angular correlation is reduced to its "hard-core" value, any increase in rf-amplitude merely results in a broadening of the resonance. This is demonstrated in Fig. 9. A comparison between the expected resonance width $\Delta y = \Delta\omega/\omega_0$ and the natural line width $\Gamma = \hbar/\tau$ is very interesting. For the 75 keV-level of ^{100}Rh the natural width is $\Gamma = 0.47$ MHz and correspondingly $\Delta y^{nat}(^{100}\text{Rh in Fe}) = 5.3 \times 10^{-4}$. It is obvious from Figs. 8 and 9 that in case of $-\omega_0\tau = 10^3$ a resonance width comparable to this natural line width can only be observed for $G_{22}^0 \gtrsim 0.9$ $(H_1/H_0 < 2.5 \times 10^{-4})$, and the effect is very small. For a more practical size of the resonance effect the expected line width is considerably wider than the natural width. From Fig. 9 it can be seen that for $H_1/H_0 = 10^{-3}$ the theoretical width of the resonance is $\Delta y = 4 \times 10^{-3}$ or

about $7.5 \cdot \Delta y^{nat}$, while for $H_1/H_0 = 10^{-2}$ one finds $\Delta y = 4 \times 10^{-2}$ corresponding to $75 \cdot \Delta y^{nat}$. After saturation (hard-core) is reached, the only effect of a power increase is a tremendous line broadening.

The fact that the line width observed in angular correlation NMR is for any reasonably sized effect far greater than the natural line width characterizes the basic difference between this technique and, e.g., Mössbauer absorption and conventional NMR measurements. While the latter two are pure energy measurements, the angular correlation involves phase relations between two successive transitions. Perturbing interactions cause both a change of the energy of the system and introduce new phase factors. Only in the limit of a vanishing perturbation, if the phase factors are small, one approaches the natural line width, but large phase factors lead to broad resonances unrelated to the natural width.

V. SUMMARY

Following the first notice[7] that NMR detection by angular correlations is possible some further experimental results are reported in the present paper. The theory was outlined briefly for the simplest geometry and a qualitative understanding of the data was reached.

The accuracy of angular correlation NMR is greatly superior to conventional PAC measurements. A search for possible candidates, however, shows that there are, in radioactive decays, only a few levels with proper half-lives suitable for this technique. Thus, in connection with angular correlations

from radioactive sources its importance will remain limited. The major application will be for isomeric states populated in nuclear reactions.[20] The generally non-isotropic angular distribution of gamma rays emitted in the decay of the product nuclei can be used to detect the resonance. The basic formalism outlined above applies for angular distribution NMR as well.

ACKNOWLEDGMENT

The skillful and dependable source preparation by Mrs. W. Heppler is gratefully acknowledged. Dr. Melvin P. Klein is also thanked for his participation in some of the early stages of this work. Helpful discussions with Professor R. M. Steffen are appreciated.

Footnote and References

1. See, e.g., S. G. Cohen, Ch. 12, p. 553, and E. Matthias, Ch. 13, p. 595, in "Hyperfine Interations," ed. by A. J. Freeman and R. B. Frankel, Academic Press, New York, 1967.
2. H. J. Körner, to be published.
3. D. A. Shirley, S. S. Rosenblum, and E. Matthias, to be published.
4. E. Matthias, D. A. Shirley, J. S. Evans, and R. A. Naumann, Phys. Rev. 140, B264(1965).
5. See, e.g., A. M. Portis and R. H. Lindquist, in "Magnetism," Vol. IIA, p. 357, ed. by G. T. Rado and H. Suhl, Academic Press, Inc., New York, 1965.
6. A. Abragam and R. V. Pound, Phys. Rev. 92, 943 (1953).
7. E. Matthias, D. A. Shirley, M. P. Klein, and N. Edelstein, Phys. Rev. Letters 16, 974 (1966).
8. Skin depth in cm: $\delta(\mathrm{Ni}) = 1.4/\sqrt{\nu}$, $\delta(\mathrm{Fe}) = 1.1/\sqrt{\nu}$.
9. R. M. Steffen and H. Frauenfelder, in Perturbed Angular Correlations, Ed. by E. Karlsson, E. Matthias, and K. Siegbahn (North-Holland Publishing Company, Amsterdam, 1964), Chapter 1.
10. V. Jaccarino, L. R. Walker, and G. K. Wertheim, Phys. Rev. Letters 13, 752 (1964)
11. M. Kontani and J. Itoh, J. Phys. Soc. Japan 22, 345 (1967).
12. W. Easley, N. Edelstein, M. P. Klein, D. A. Shirley, and H. H. Wickman, Phys. Rev. 141, 1132 (1966).
13. S. G. Schmelling, V. J. Ehlers, and H. A. Shugart, Phys. Rev. 154, 1142 (1967).

14. J. Eisinger and V. Jaccarino, Rev. Mod. Phys. 30, 530 (1958).

15. N. Kaplan, V. Jaccarino, and J. H. Wernick, Phys. Rev. Letters 16, 1142 (1966).

16. J. Budnick, private communication.

17. See, e.g., A. Abragam, The Principles of Nuclear Magnetism, Oxford University Press, Oxford, 1961, and C. P. Slichter, Principles of Magnetic Resonance, Harper's Physics Series, Harper and Row, New York, 1963.

18. Eq. (7) is only correct for circularly polarized rf. We follow the common p-axis that linearly polarized rf can be described as a superposition of two opposite circularly polarized components, only one of which actually induces resonance transitions.

19. E. Matthias, S. S. Rosenblum, and D. A. Shirley, Phys. Rev. Letters 14, 46 (1967).

20. R. M. Diamond, E. Matthias, J. O. Newton, and F. S. Stephens, Phys. Rev. Letters 16, 1205 (1966).

Table I. Summary of resonance frequencies obtained for ^{100}Rh in Fe with different sources and different power levels.

source no	temperature (°K)	ν_R(MHz)	width (MHz)	effect (%)	average power (watts)
1	300	882.7±2.0	~7	3.8	80
2	300	881.7±1.0	~6	2.5*	50
3	300	883.4±1.3	~8	0.8*	20
4	77	912.5±1.0	~7	2.1*	50

*not corrected for accidental coincidences.

Figure Captions

Fig. 1. Sketch of the geometry of a resonance experiment with angular correlations.

Fig. 2. Resonance effect for ^{100}Rh in Fe at room temperature (source no. 1 in Table I). The polarizing field was 385 gauss and the average power was 80 watts.

Fig. 3. Saturation behavior of the foil as a function of the polarizing field without rf-field and with 100 watts power at resonance frequency.

Fig. 4. Power dependence of the magnitude of the effect at resonance. The power range extends from 0 to 100 watts.

Fig. 5. Resonance effect for ^{100}Rh in Fe at two different temperatures. The polarizing field was 100 gauss and the rf amplitude was about 1.5 gauss. The data points are not corrected for accidental coincidences.

Fig. 6. Resonance effect for ^{100}Rh in Ni at room temperature. The polarizing field was 450 gauss and the average power was 35 watts.

Fig. 7. Typical resonance curves for some realistic parameters H_1/H_0 and $\omega_0\tau$ in the case of a spin I=2.

Fig. 8. Theoretical power dependence of the perturbation factors $\hat{G}_{kk}^{00}$ at resonance. $\hat{G}_{22}^{00}$ is shown for two realistic values of $\omega_0\tau$.

Fig. 9. Theoretical dependence of the shape of the resonance on the rf-amplitude.

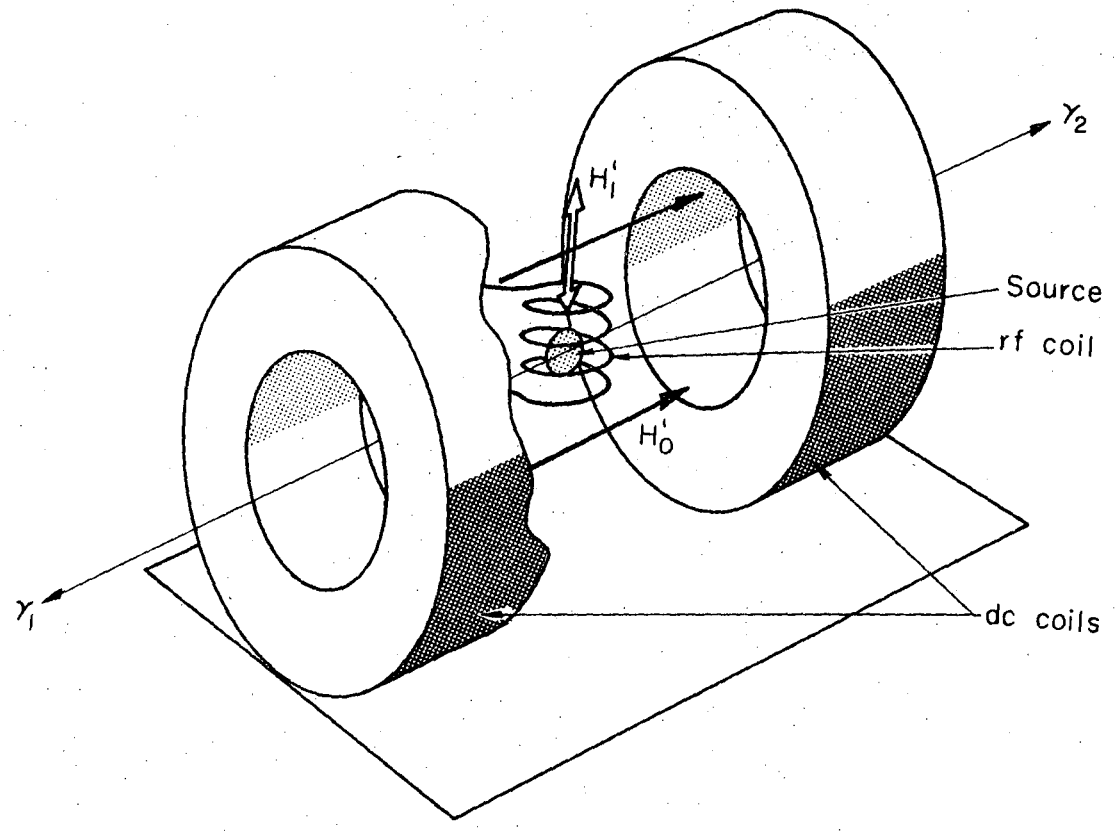

Fig. 1

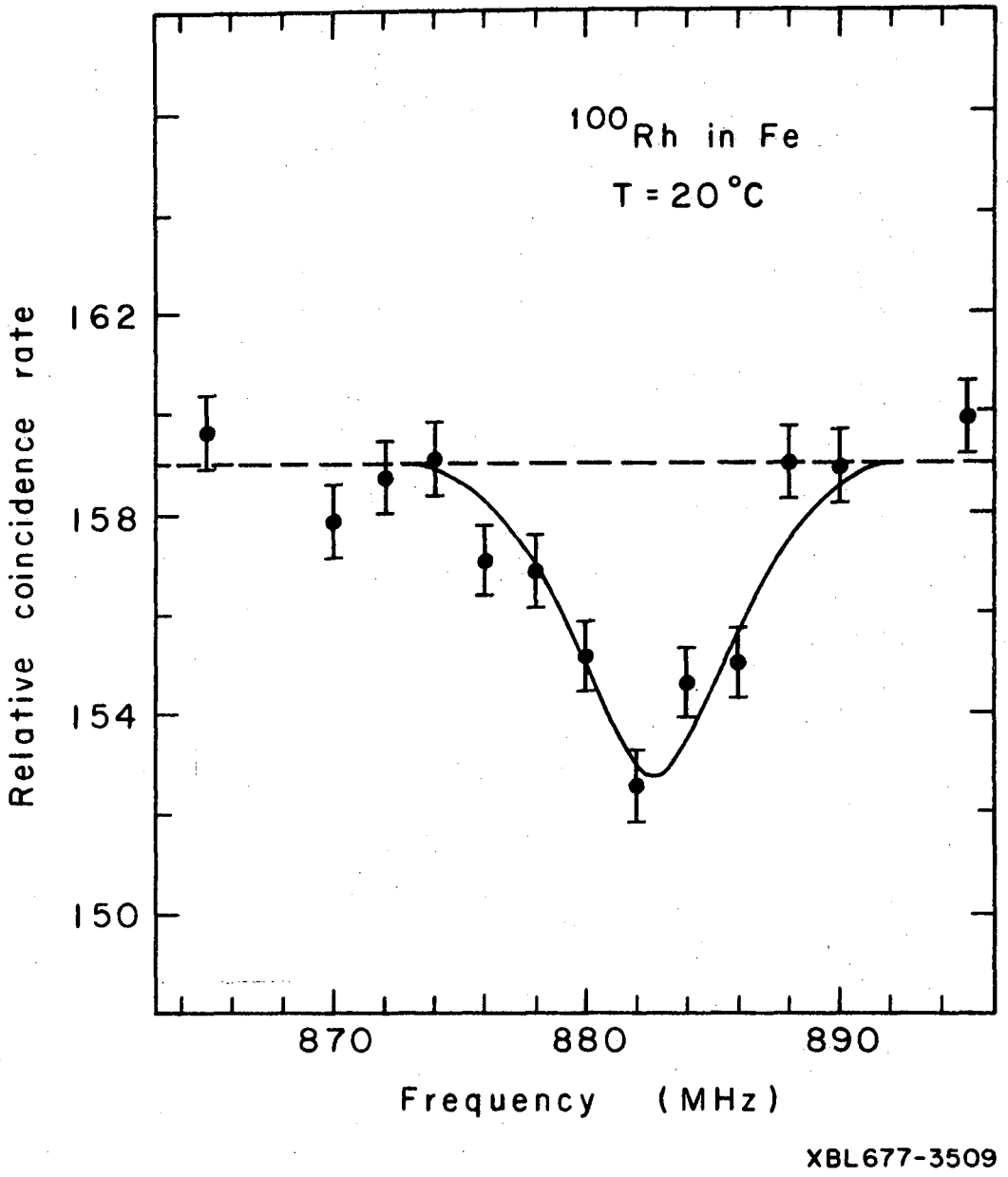
^{100}Rh in Fe
T = 20°C
Relative coincidence rate
162
158
154
150
870
880
890
Frequency (MHz)
XBL677-3509

Fig. 2

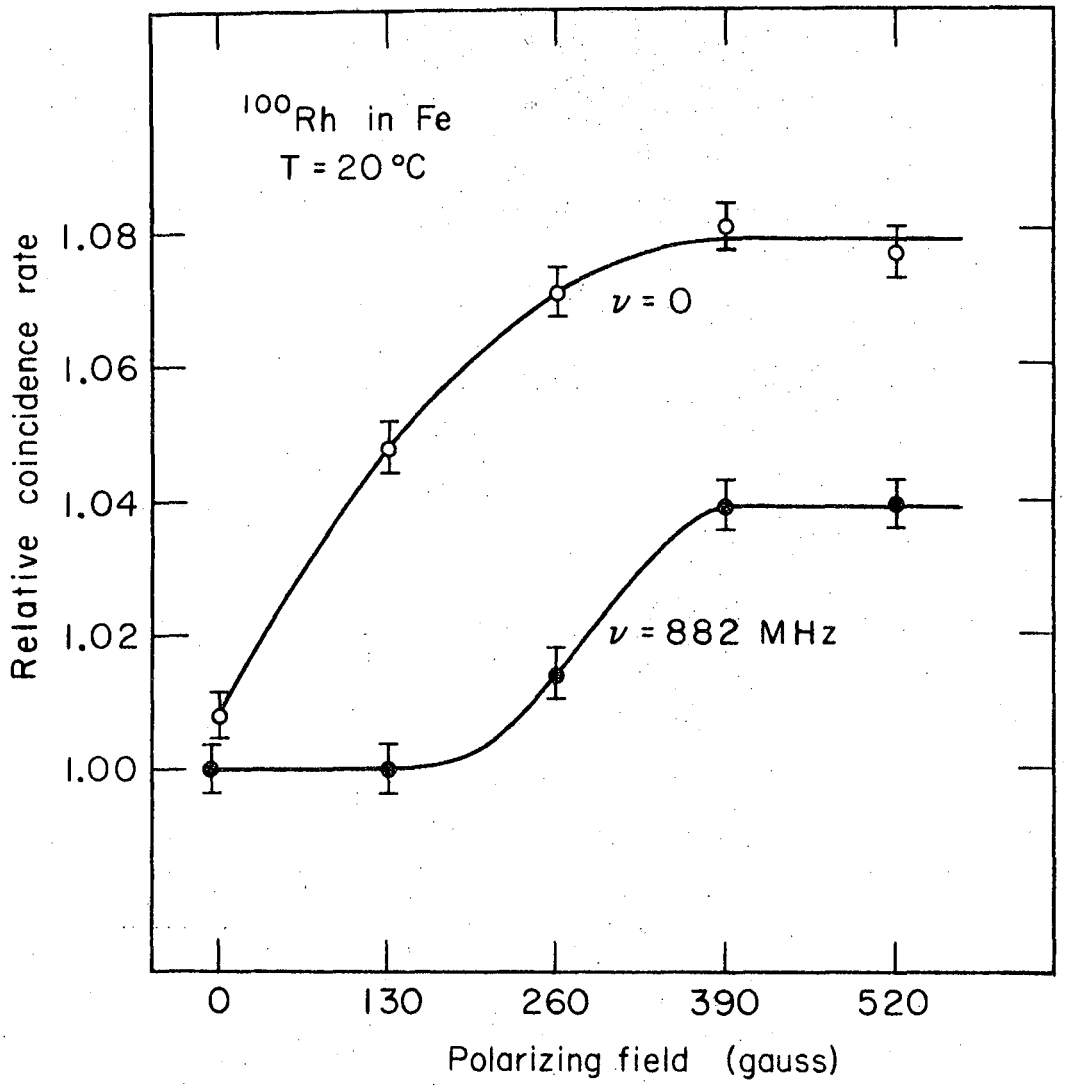
^{100}Rh in Fe
T = 20 °C
Relative coincidence rate
1.08
1.06
1.04
1.02
1.00
ν = 0
ν = 882 MHz
0
130
260
390
520
Polarizing field (gauss)
MUB 13766-A

Fig. 3

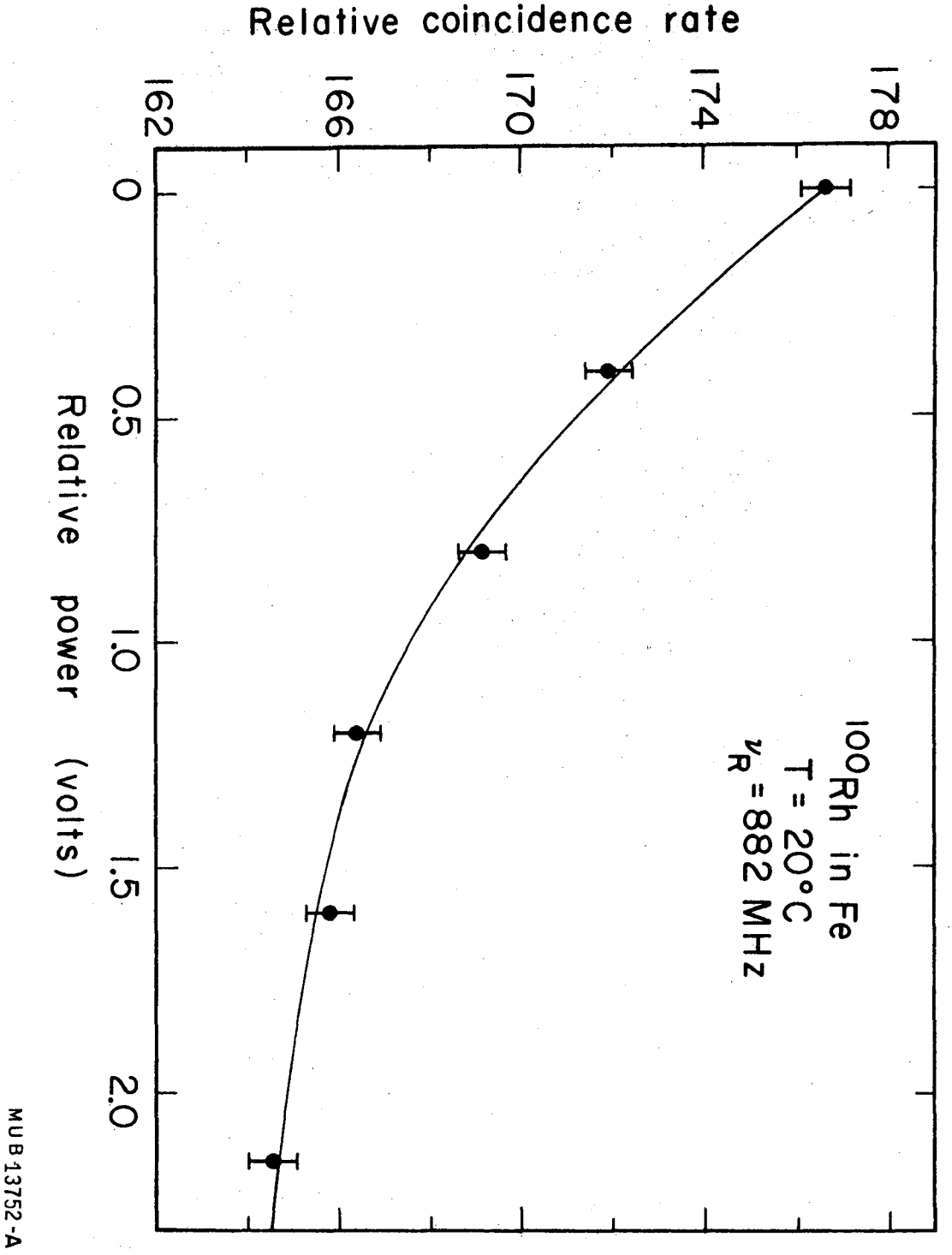
Relative coincidence rate
162
166
170
174
178
0
0.5
1.0
1.5
2.0
Relative power (volts)
100Rh in Fe
T = 20°C
νR = 882 MHz
MUB 13752-A

Fig. 4

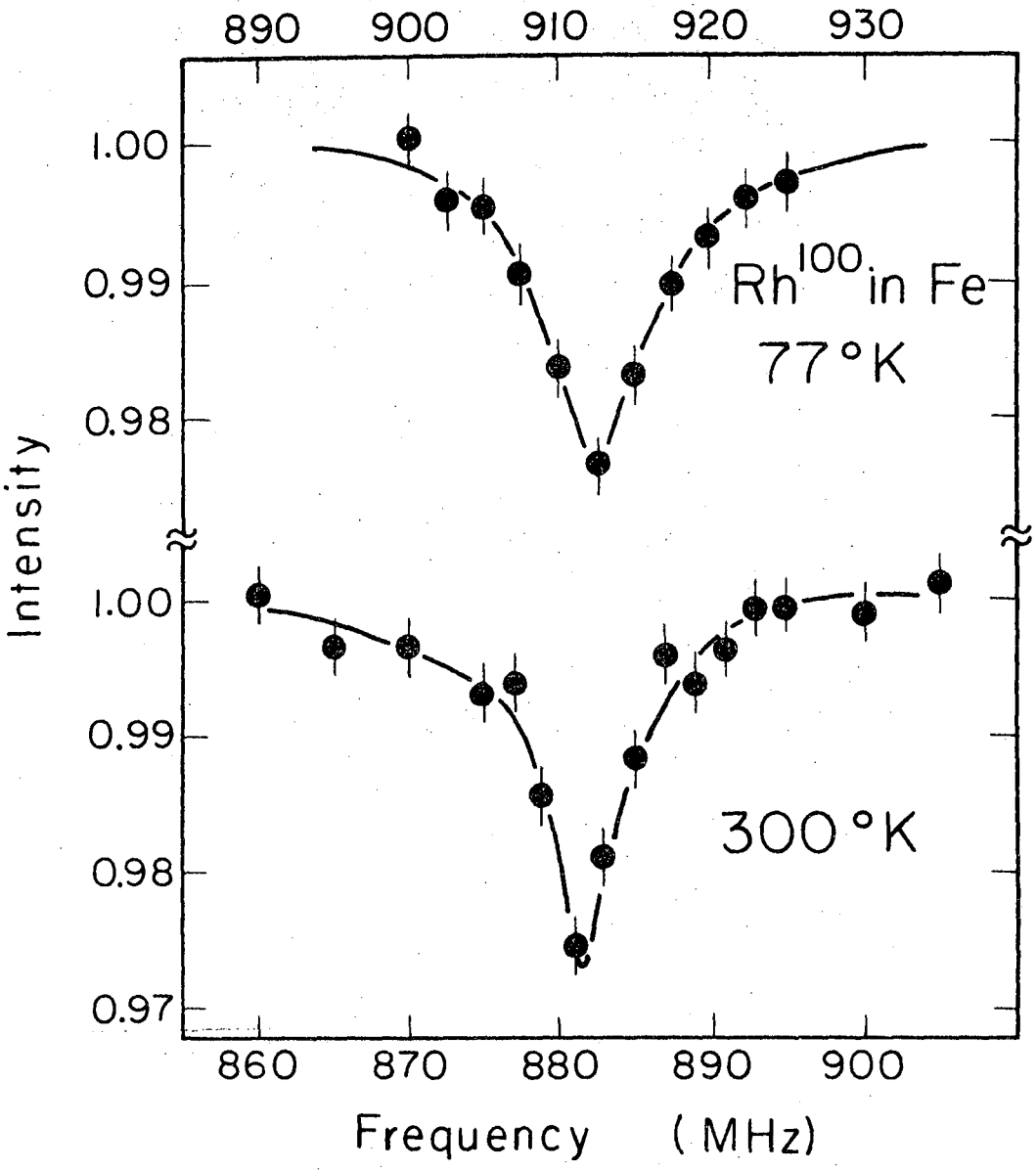

MUB-11913

Fig. 5

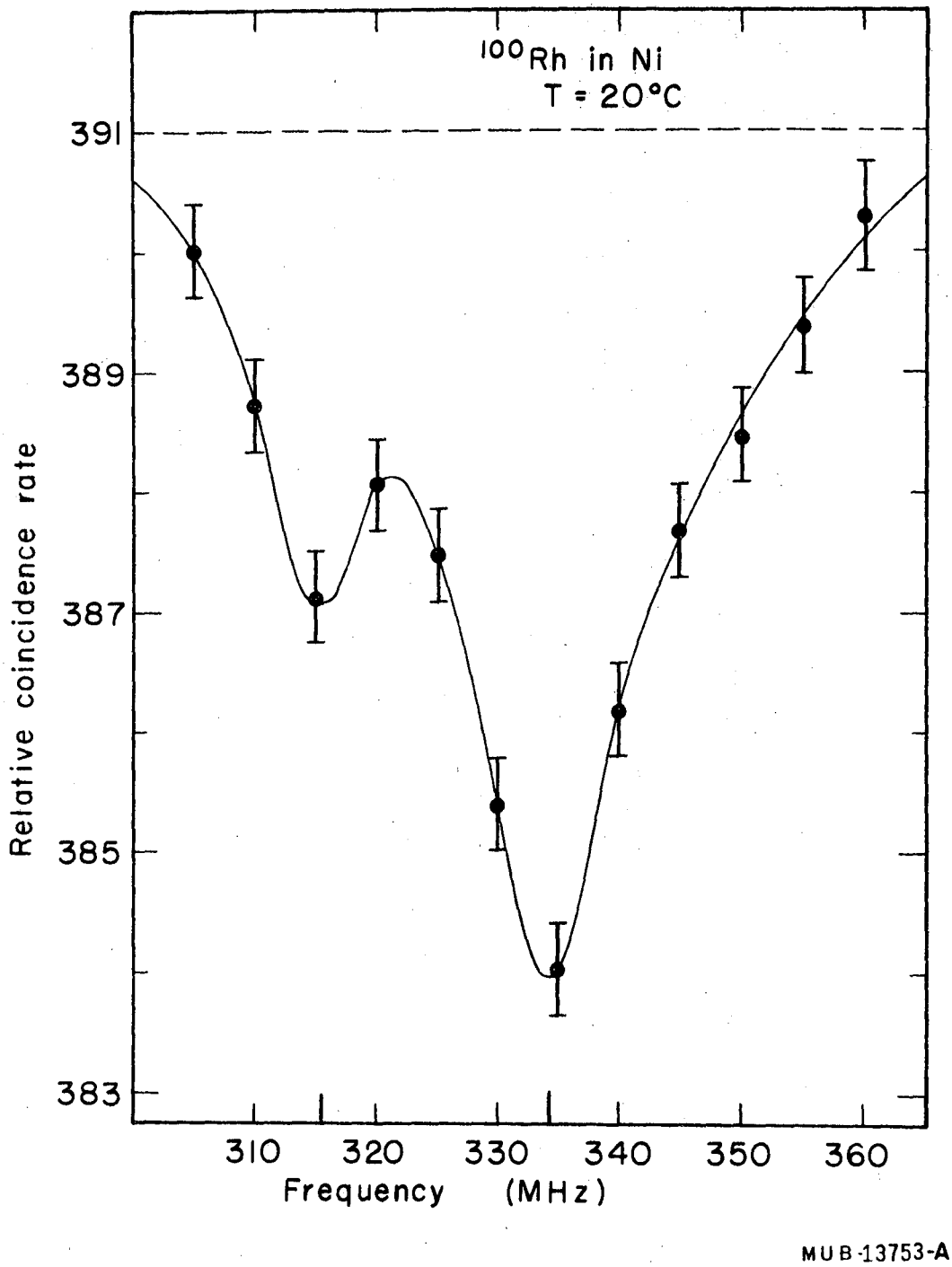
^{100}Rh in Ni
T = 20°C
391
389
387
385
383
Relative coincidence rate
310
320
330
340
350
360
Frequency (MHz)
MUB-13753-A

Fig. 6

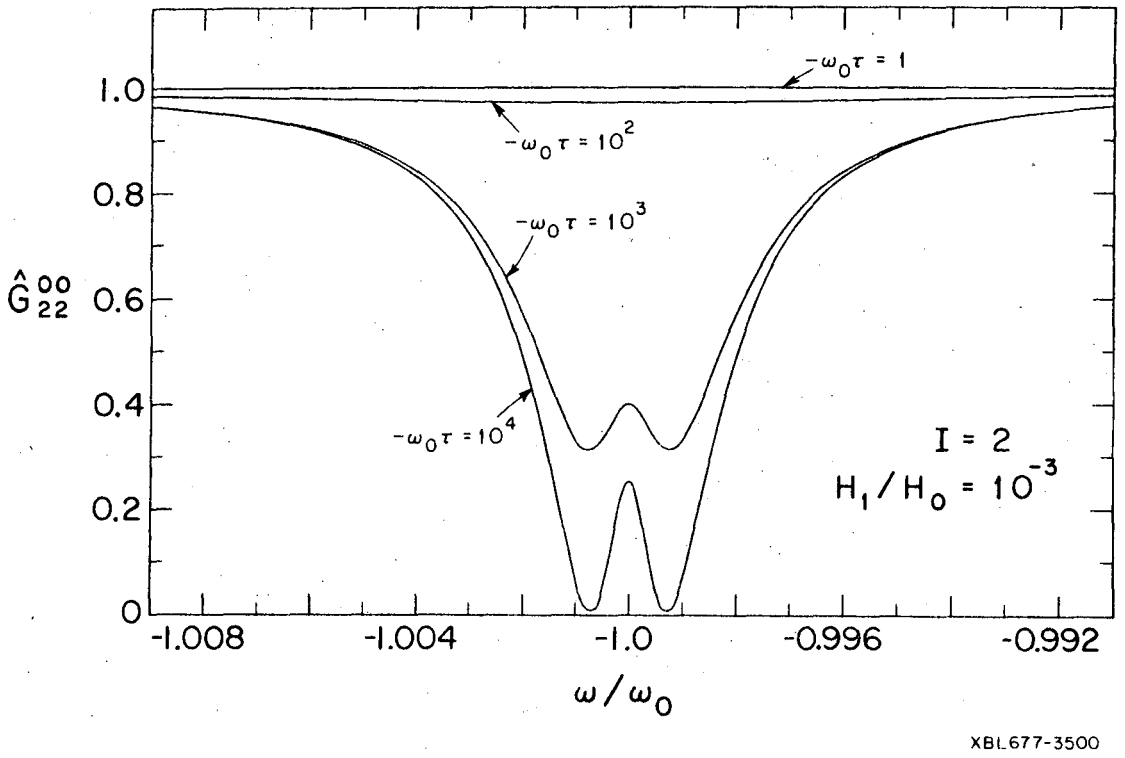
$-\omega_0\tau = 1$
$-\omega_0\tau = 10^2$
$-\omega_0\tau = 10^3$
$-\omega_0\tau = 10^4$
I = 2
$H_1/H_0 = 10^{-3}$
$\hat{G}^{00}_{22}$
1.0
0.8
0.6
0.4
0.2
0
-1.008
-1.004
-1.0
-0.996
-0.992
ω/ω_0
XBL677-3500

Fig. 7

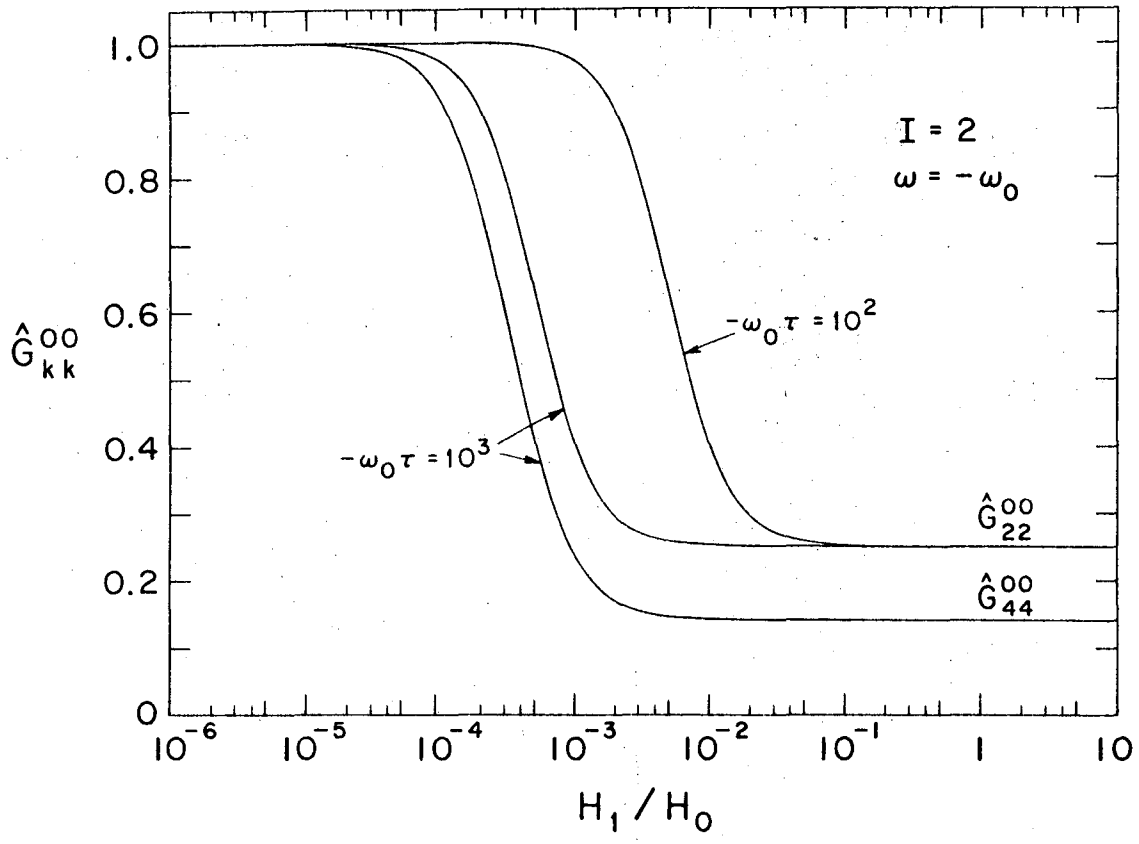

XBL677-3499

Fig. 8

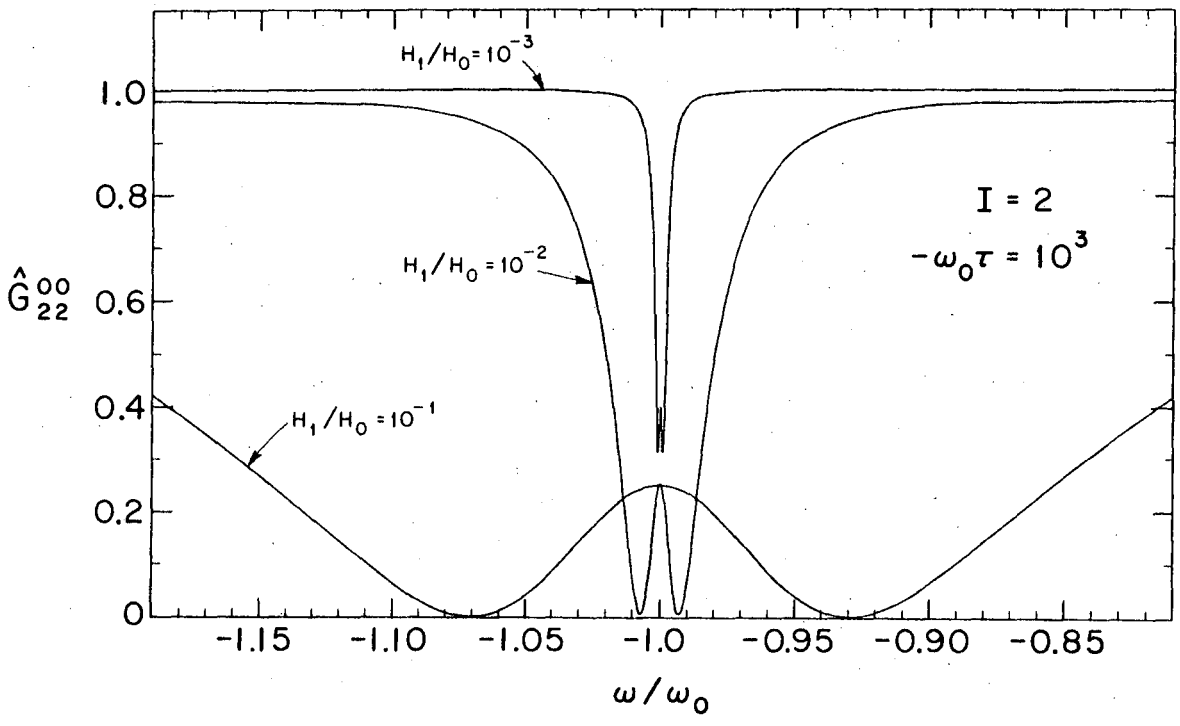
$H_1/H_0 = 10^{-3}$
$H_1/H_0 = 10^{-2}$
$H_1/H_0 = 10^{-1}$
I = 2
$-\omega_0\tau = 10^3$
$\hat{G}^{00}_{22}$
1.0
0.8
0.6
0.4
0.2
0
-1.15
-1.10
-1.05
-1.0
-0.95
-0.90
-0.85
ω/ω_0
XBL677-3498

Fig. 9